Common load suppressed stochastization mediated by noise

A.L. Pankratov[1,2,3], E.V. Pankratova[3], V.A. Shamporov[3], S.V. Shitov[4,5]
[1] *Institute for Physics of Microstructures of RAS, Nizhny Novgorod, Russia*
[2] *Cryogenic Nanoelectronics Center, Nizhny Novgorod State Technical University n.a. R.E. Alexeyev, Nizhny Novgorod, Russia*
[3] *N.I. Lobachevsky State University of Nizhni Novgorod, Nizhny Novgorod, Russia*
[4] *Institute of Radio-engineering and Electronics of RAS, Moscow, Russia*
[5] *Laboratory of Superconducting Metamaterials, National University of Science and Technology "MISIS", Moscow, Russia*

The joint action of the matching to a common RC-load and thermal noise on the spectral properties of phase oscillators arrays is studied. It is demonstrated that proper matching may suppress the chaotic dynamics of the system. The efficiency of radiation was found to be highest within a limited frequency band, which corresponds to transformation of the shuttle soliton oscillating regime into the linear wave resonance synchronization mode. In this frequency band the spectral linewidth agrees well with a double of the linewidth for a shuttle fluxon oscillator, divided by a number of the oscillators in the chain. If the oscillations demonstrate strong amplitude modulation, it leads to increase of the linewidth roughly by a factor of five compared to this theoretical linewidth formula.

The dynamics of systems where the nonlinear active elements interact with each other through additional external media can demonstrate surprising properties of collective behavior. Such coupling is widely spread in nature and technology and describes, for example, vibrations of a common base supporting oscillating mechanical systems [1, 2], concentration of chemicals that diffuse in the surrounding medium and provide the coupling in biological populations [3–5], electromagnetic field interacting with the cold atoms [6], common dynamic environment indirectly linking the electronic circuits [7], etc. The regimes observed in such systems are highly diverse, varying from different types of oscillation quenching to a multitude of synchronous regimes [1, 7, 8]. Namely, synchronous regimes in the common base-coupled mechanical systems can drastically enhance vibrations of the base leading to destruction of the latter [9]. Moreover, the environmental coupling can significantly change the dynamical characteristics leading to birth of complicated chaotic and hyperchaotic regimes of oscillations. Particularly, for the mechanical self-excited nonlinear oscillators coupled through a common beam the conditions for a wild attractor were obtained in Ref. [10], while accounting for environmental noise can modify the dynamics via new mechanisms of coherent generation development [11]. Therefore, the investigation of the joint effect of noise and a common load on the dynamics of complex networks is of general importance for a wide spectrum of tasks. In this Letter, we consider this problem in the frame of the Frenkel-Kontorova model [12, 13]

$$\ddot{\phi}_j + \alpha\dot{\phi}_j + \sin\phi_j = i_{dc} + i_f(t) + \varepsilon(\phi_{j-1} - 2\phi_j + \phi_{j+1}), \quad (1)$$

that has a broad variety of mechanical, chemical, biological and physical applications including DNA-promoter dynamics [14], magnetic domain wall racetrack memory [15], digital circuits [16] and ballistic detectors [17, 18] based on Josephson junctions (JJs). In Eq. (1) ϕ_j is the phase of the j-th oscillator, α and ϵ are the damping and the coupling parameters, respectively. Each oscillator is biased by an external force i_{dc} and subjected to fluctuations $i_f(t)$, which we assume to be white Gaussian noise with the dimensionless noise intensity γ: $\langle i_f(t) i_f(t+\tau)\rangle = 2\alpha\gamma\delta(\tau)$. We consider the chain with the RC-load [19, 20]: $di_R/dt = -i_R/r_R c_R + \ddot{\phi}_n(t)/r_R$, where $i_R(t)$ is the alternating current through the right load, r_R and c_R - right load dimensionless resistance and capacitance; the similar equation can be written for the left load with r_L and c_L. Particularly, for Josephson applications the considered system describes the dynamics in a parallel JJ array (JJA) shown in Fig. 1, where crosses denote JJs with their internal capacitance, resistance and nonlinear inductance, $\epsilon = 1/l$ is the inverse inductance between JJs and i_{dc} is the bias current.

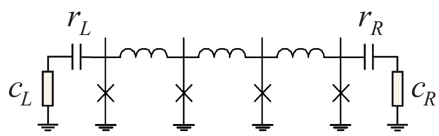

Figure 1: An example of a parallel chain with RC-loads.

The increasing interest to the Josephson effect is associated with its THz applications. The weak radiation power of a single junction had motivated a study of the processes of synchronization of various JJ arrays [21–28], with the aim to increase the radiation power; for example, in Ref. [25] a high-efficiency serial-parallel 2-D array of JJs was fabricated and studied. The remarkably high efficiency of

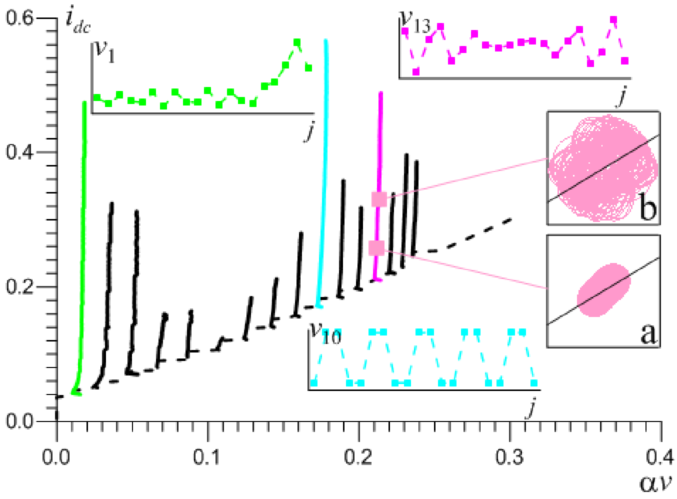

Figure 2: Current-voltage characteristics for the JJ array with weakly coupled load $r_L = 30$; dashed curve corresponds to return-path IVC, steep solid curves are steps, corresponding to direct-path IVCs. Insets demonstrate the voltage distribution $v_k = d\phi_j(t)/dt$ at a fixed point in time versus the junction number, j, for the steps $k = 1, 10, 13$; the two phase portraits for unmatched case $c_L = c_R = 0$ at: a) $i_{dc} = 0.26$, b) $i_{dc} = 0.33$.

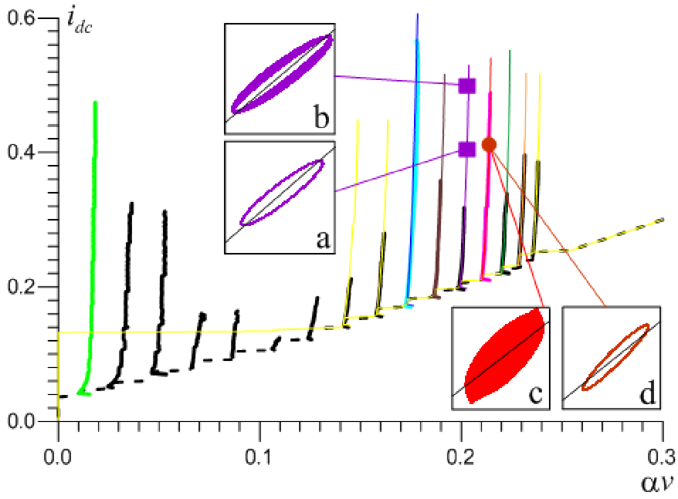

Figure 3: Current-voltage characteristics for the matched JJ array. Thin yellow and colored curves correspond to return and direct-path IVCs for the matched RC load $r_L = 2$, while other curves are the same as in Fig. 2. Insets show phase portraits at corresponding points of IVCs: a) $i_{dc} = 0.41$ and b) $i_{dc} = 0.49$ for $r_L = 2$; c) $r_L = 2$ and d) $r_L = r_R = 1$ for $i_{dc} = 0.41$.

radiation and a clear threshold of generation have been discussed in a few papers, but have not been completely understood yet. The authors of Ref. [25] have suggested the internal cell resonance to be responsible for the oscillating frequency. Ref.s [27, 28] have qualitatively shown that a similar threshold effect of radiation is observed if a chain of JJs is coupled to a high-Q cavity load. However, in real applications [29] one desires a broader frequency range for an oscillator that corresponds to a lower-Q. To address this problem, an RC-load is usually placed at only one end of the chain [25]; however, due to the distributed nature of a JJ transmission line, this leads to a possibility that not all JJs in the chain are coupled equally to the load (unlike the cases of high-Q loads, as treated theoretically). This illustrates the lack of detailed understanding of the synchronism in real JJA.

We have performed an investigation of the spectral characteristics of radiation from a JJA, the output power and linewidth, at different steps of its current-voltage characteristics (IVC). For experimentally relevant parameters $\alpha = 0.03$, $\varepsilon = 4.41$ and number of junctions $n = 20$ the system (1) has been solved numerically. The dependence of time averaged voltage $v = \overline{d\phi(t)/dt}$ on the injected current i_{dc} is presented in Fig. 2 for zero noise intensity, a weakly matched load at the left end ($r_L = 30$, $c_L = 100$) and an unmatched load at the right end ($r_R = 100, c_R = 100$). The load capacitance is sufficiently large, and allows for transmission of power to the load resistance at all frequencies of interest. For small currents $i_{dc} \to 0$ the system remains in the superconducting state. At large currents, $i_{dc} > 0.6$, the behavior is ohmic, i.e. the voltage is proportional to the characteristic resistance $v = i_{dc}/\alpha$.

The first step of the IVC corresponds to the mode with a single soliton moving along the chain [24]. At the second and the third steps two and three moving solitons can be distinguished. At 4-th and 5-th steps the behavior appears chaotic; the reason of this may either be destructive interference of linear waves, or a combination of effects of restricted length of the system ($\sim 10\lambda_J$) and the discreteness of the chain. Here, one can also observe the minor steps at IVCs due to Cherenkov radiation of moving solitons [18, 24, 31–33]. At the weakly biased higher-order steps the voltage oscillations have the form of standing waves (see the inset with $v_{10}(j)$ for 10-th step in Fig. 2) with the amplitude significantly exceeding that of the first three steps. It is worth noting that in the completely unmatched case ($c_L = c_R = 0$), at the top of 12-th and higher-order steps the Ruelle-Takens-Newhouse scenario [30] of transition from periodic to quasi-periodic oscillation (inset (a) in Fig. 2) to chaos (inset (b) in Fig. 2) is observed, while the chaotic behavior disappears even at weak matching at one end, $r_L = 30$, for which Fig. 2 is plotted.

If a matched load is placed at one end of the chain

($r_L = 2$, $c_L = 100$, while $r_R = 100$, $c_R = 100$), the IVCs for higher steps (8th-16th, shown as thinner, colored curves in Fig. 3) change drastically. As seen from Fig. 3, the role of matching is crucial: all steps below 8-th disappear, which means that few-soliton trains leave the chain, absorbed by the load. Moreover, the higher-order steps become taller (with respect to i_{dc}) and the dynamics at their tops changes significantly: the amplitude modulation regimes shift to larger values of bias current, the chaotic regimes do not evolve (the oscillations become more regular in comparison with unmatched case). The phase portrait calculated for zero noise intensity $\gamma = 0$ at 12th step for bias currents $i_{dc} = 0.41$ (inset a) in Fig. 3) demonstrates the limit cycle corresponding to a purely periodical oscillations; the regimes with amplitude modulation observed at 12th (for $i_{dc} = 0.49$) and 13th (for $i_{dc} = 0.41$) steps are depicted in Fig. 3 within the insets b) and c), respectively. The inset d) in Fig. 3 illustrates the amplitude modulation vanishing as a result of better load matching. In the presence of small noise $\gamma \leq 0.1$, the IVCs for steps are roughly the same as in the zero-noise case (data not shown).

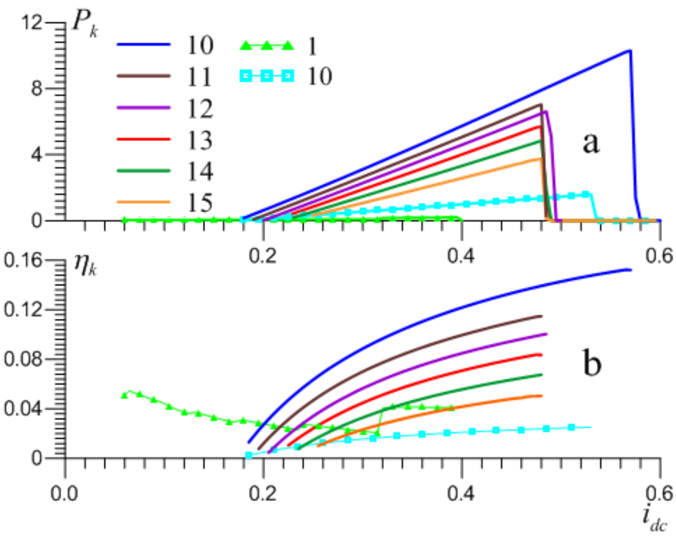

Figure 4: Variation of a) - the radiation power at the left load P_k and b) - the radiation efficiency η_k vs bias current for k-th step of IVC; solid curves for $r_L = 2$, $r_R = 100$, curves with symbols for $r_L = 30$, $r_R = 100$.

The radiation power at the left load versus bias current, shown in Fig. 4a for the weakly matched load and noise intensity $\gamma = 0.05$, resembles the behaviour of experimental data [25]: the power at first six steps is weak, of the order of the first step power, while for higher steps the increase of the radiation power is observed (data for steps 1 and 10 are shown by symbols). For the matched RC-load the oscillation power grows linearly with the increase of bias current i_{dc}, which is a well-known dependence obtained in experiments with flux-flow oscillators [29], and varies twofold throughout steps 8 to 15, reaching its maximum at the 10th step. One can find the ratio η of the ac power to the dc power, see Fig. 4b. It should be noted that for the 10th step with a matched load we get nearly the same efficiency as in experiment [25]. Such an increase in power is accompanied by the transition from zero-field steps to the resonant Fiske modes (see IVCs at Fig. 2, 3), which is characterized by the change of distances between steps from almost $3\pi/L$ at first steps to $2\pi/L$ around 10th step and to π/L around 15th step. This effect can be explained by the constructive interference of linear waves in a resonator formed by the whole chain and its load.

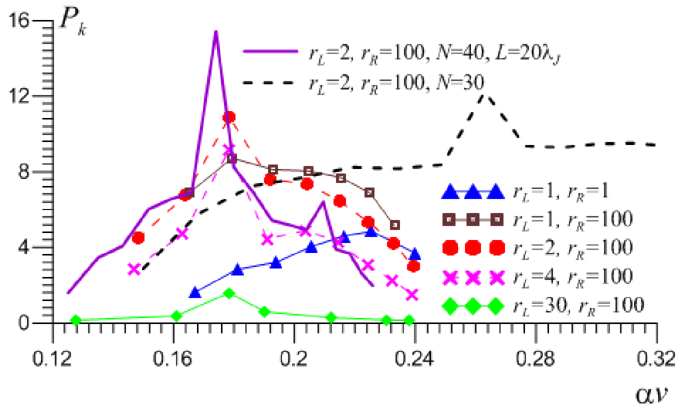

Figure 5: The radiation power P_k of oscillations vs voltage for various matching of RC load and number of junctions.

The maximal generated power P_k transferred to the left end at the k-th step of the IVC, is plotted versus the voltage in Fig. 5 for various matching of RC load. It reveals the existence of a frequency band where radiation is more efficient. While improving the matching at one end increases the power significantly without shifting the optimal frequency range, proper matching at both ends of the chain leads to the shift of maximum power to higher frequencies. In the latter case one should take into account that power is extracted from both ends of the array, so the total power is double of what is presented on the graph. The maximal generation efficiency reaches 15% for the load $r_L = 2$, $r_R = 100$. Increasing the number of junctions in the chain with fixed chain length to $N = 30$ shifts the optimal frequency range by a factor of 1.5, increases the power, but decreases the efficiency η_k. Increasing both the number of junctions $N = 40$ and length $L = 20\lambda_J$ (i.e. keeping the coupling ϵ the same) increases the power at the optimal point, but decreases it for higher frequencies, thus confirming the mechanism of powerful generation as interference of linear waves in a resonator formed by the array and its load.

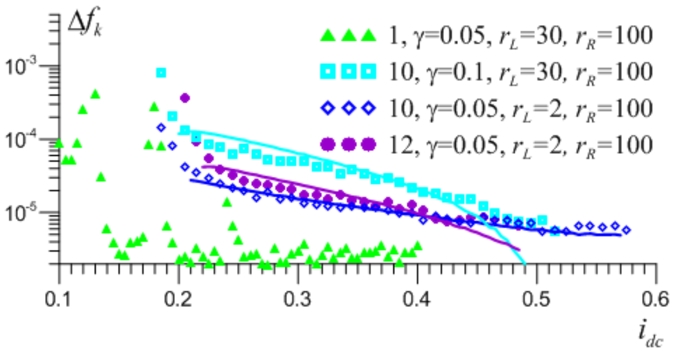

Figure 6: Spectral linewidth Δf_k vs bias current i_{dc} for k-th step of IVC; solid curves denote theory (2).

The curves of spectral linewidth of radiation versus bias current i_{dc} are shown in Fig. 6. It should be noted that the linewidth at zero field steps is by about two or three orders of magnitude smaller than the linewidth at flux-flow steps [34, 35] at the same damping. This requires simulations with much better spectral resolution and therefore takes much more calculation time. The difference in linewidth is presumably due to the smaller dissipation in a zero field regime, which is reflected by the much smaller differential resistance at zero field steps than at flux-flow steps. Comparing the calculated linewidth with the analytical formulas for the single JJ [36] and the shuttle fluxon oscillator [37], one can see that for the 10-th and 12-ve steps the linewidth agrees well with the analytical formula [37], multiplied by a factor of 2 and divided by the number of junctions N:

$$\Delta f = \alpha\gamma r_d^2/N. \tag{2}$$

The change of the numerical factor can be attributed to the fact that we perform the comparison not with the single-fluxon regime, but with a mixed traveling and standing wave regimes. Comparison of calculated and theoretical linewidth at the first step is, unfortunately, out of our present computational capabilities due to sharp Cherenkov steps at the IVC, which does not allow for accurate calculation of the differential resistance r_d. From Fig. 6 one can see that deviation of the calculated linewidth from theory (2) increases at the top of the 10-th and 12-th steps. This can be explained by amplitude modulation of oscillations at the tops of the steps (inset b in Fig. 3) that, in the absence of phase fluctuations, does not lead to broadening of the spectral linewidth, even if these modulations are random [38]. The presence of noise, however, leads to the diffusion of phase, which interplays with the amplitude modulation, leading to the linewidth increase and deviation from Eq. (2). Due to the strong amplitude modulation of the signal (shown, for example, in the inset c) of Fig. 3), the increase of the linewidth at higher steps is even larger: for the 13th step the peak is shown by red circles in Fig. 7. Decreasing the noise intensity γ leads to smoothing of this peak, and the linewidth increases by a factor of 5 in comparison with the formula (2). Therefore, the occurrence of a strongly pronounced peak with the increase in noise intensity confirms the non-triviality of mutual influence of fluctuations and the load on the system behavior. An improvement of matching ($r_L = r_R = 1$) makes the dynamics more regular for the entire length of the step: only the limit cycle (shown in the inset d) of Fig. 3) is observed here for varying values of i_{dc}. Furthermore, with this matching the linewidth is well described by (2), see the empty brown rectangles and the corresponding solid curve in Fig. 7.

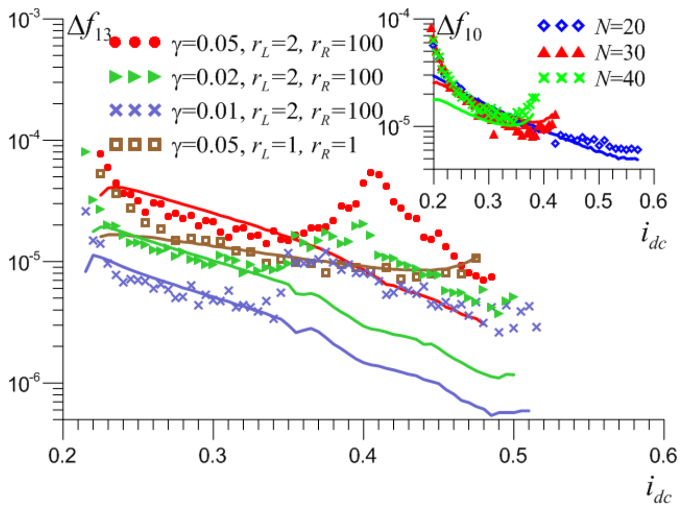

Figure 7: Spectral linewidth Δf_{13} vs bias current i_{dc} for 13th step of IVC for various values of γ and load resistance. Inset: spectral linewidth versus bias current for 10th step of IVC for various number of junctions in the chain; solid curves denote theory (2), $\gamma = 0.05$, $r_L = 2$, $r_R = 100$.

The spectral linewidth for chains with various number of junctions but the same chain length is presented in the inset of Fig. 7 for the 10th step with proper load matching $r_L = 2$, $r_R = 100$. Yet again, Eq. (2) gives reasonable agreement with the computer simulation results, since regular generation and a limit cycle in the phase space of the system is observed along the whole step.

In the present Letter we show that the threshold of radiation power and high efficiency of radiation can be observed in a simple parallel (ladder-type) JJ array with an RC load taken into account. We have demonstrated that the most efficient radiation can be anticipated within the frequency range that corresponds to transformation of the shuttle soliton oscillating regime into the linear wave resonance synchronization mode (i.e. from zero field steps into the Fiske steps at the IV-curve of the RC-loaded JJA, respectively). While we have considered the RC-load equally matched for all frequencies, in reality good matching is usually achieved at high frequencies, so the observed threshold of radiation power can be magnified. In case of a matched RC load, the radiation power is expected to reach 15% of the total dc power. Remarkably, for regular oscillation regimes at the higher-order resonant steps, the linewidth agrees well with the half of theoretical linewidth for a short Josephson junction [36] and a double of the linewidth for a shuttle fluxon oscillator [37], divided by a number of the junctions in the chain. If the oscillations demonstrate strong amplitude modulation, it leads to increase of the linewidth by a factor of five in comparison with the theory.

The authors wish to thank V. Krasnov and M. Fistul for comments and suggestions. This work is supported by RFBR (projects 14-02-31727 and 15-02-05869), by Ministry of Education and Science of the Russian Federation (projects 11.G34.31.0062, 14.740.12.0845 and 3.2054.2014/K), and in the framework of Increase Competitiveness Program of Lobachevsky NNSU under contract no. 02.B.49.21.0003 and NUST (MISiS) under contract no. K2-2014-025.

[1] M. Bennett, M. Schatz, H. Rockwood, K. Wiesenfeld, Proc. R. Soc. Lond. A **458** (2019), 563 (2002).
[2] E.V. Pankratova, V.N. Belykh, Phys. Lett. A, **376** (45), 3076 (2012).
[3] D. Gonze, S. Bernard, C. Waltermann, A. Keamer, H. Herzel, Biophys. J. **89**, 120 (2005).
[4] K. Kruse, F. Julicher, Curr. Opin. Cell Biol. **17**, 20 (2005).
[5] G. Katriel, Physica D **237**, 2933 (2008).
[6] J. Javaloyes, M. Perrin, A. Politi, Phys. Rev. E **78**, 011108 (2008).
[7] R. Suresh, K. Srinivasan, D. V. Senthilkumar, K. Murali, M. Lakshmanan, and J. Kurths, Int. J. of Bif. and Chaos. **24** (5), 1450067 (2014).
[8] V. Resmi, G. Ambika, R. E. Amritkar, and G. Rangarajan, Phys. Rev. E **85**, 046211 (2012).
[9] S.H. Strogatz, D.M. Abrams, A. McRobie, B. Eckhardt, E. Ott., Nature **438** (7064), 43 (2005).
[10] V.N. Belykh, E.V. Pankratova, Int. J. of Bif. and Chaos **24** (8), 1440007 (2014).
[11] E.V. Pankratova, V.N. Belykh, Europ. Phys. J. Special Topics **222**, 2509 (2013).
[12] O.M. Braun, Yu.S. Kivshar, *The Frenkel-Kontorova Model: Concepts, Methods, and Applications* (Springer-Verlag, Berlin, 2004).
[13] Y.S. Kivshar, B.A. Malomed, Rev. Mod. Phys. **61**, 763 (1989).
[14] M. Salerno, Phys. Rev. A 44, 5292 (1991); M. Salerno and Yu. S. Kivshar, Phys. Lett. A 193, 263 (1994); L.V. Yakushevich, A.V. Savin, and L. I. Manevitch, Phys. Rev. E 66, 016614 (2002).
[15] S.S.P. Parkin, M. Hayashi, and L. Thomas, Science 320, 190 (2008).
[16] K.K. Likharev and V.K. Semenov, IEEE TAS 1, 3 (1991).
[17] V.K. Semenov and D.V. Averin, IEEE TAS 13, 960 (2003).
[18] I.I. Soloviev, N.V. Klenov, A.L. Pankratov, E. Il'ichev, and L.S. Kuzmin, Phys. Rev. E **87**, 060901(R) (2013).
[19] C. Soriano, G. Costabile, and R.D. Parmentier, Supercond. Sci. Technol. **9**, 578 (1996).
[20] A.L. Pankratov, A.S. Sobolev, V.P. Koshelets, and J. Mygind, Phys. Rev. B **75**, 184516 (2007).
[21] A.K. Jain, K.K. Likharev, J.E. Lukens, J.E. Sauvageau, Phys. Rep. **109** (6), 309 (1984).
[22] S.G. Lachenmann, et al, J. Appl. Phys. **77**, 2598 (1995).
[23] P.A.A. Booi, S.P. Benz, Appl. Phys. Lett. **68**, 3799 (1996).
[24] A.V. Ustinov, B.A. Malomed, S. Sakai, Phys. Rev. B **57**, 11691 (1998).
[25] P. Barbara, A. B. Cawthorne, S. V. Shitov and C. J. Lobb, Phys. Rev. Lett. **82**, 1963 (1999).
[26] D. Abraimov, P. Caputo, G. Filatrella, M.V. Fistul, G.Yu. Logvenov, and A.V. Ustinov, Phys. Rev. Lett. **83**, 5354 (1999).
[27] G. Filatrella, N.F. Pedersen, and K. Wiesenfeld, Phys. Rev. E **61**, 2513 (2000); IEEE TAS **11**, 1184 (2001).
[28] G. Filatrella, B. Straughn, P. Barbara, J. Appl. Phys. **90**, 5675 (2001).
[29] V.P. Koshelets and S.V. Shitov, Supercond. Sci. Technol. **13**, R53 (2000).
[30] D. Ruelle, F. Takens, Commun. Math. Phys. **20**, 167 (1971); J.-P. Eckmann, Rev. Mod. Phys. **53**, 643 (1981).
[31] A.V. Ustinov, M. Cirillo, and B.A. Malomed, Phys. Rev. B **47**, 8357 (1993).
[32] A.V. Ustinov, M.Cirillo, B.H. Larsen, V.A. Oboznov, P. Carelli, and G. Rotoli, Phys. Rev. B **51**, 3081 (1995).
[33] O.M. Braun, B. Hu, A. Zeltser, Phys. Rev. E **62**, 4235 (2000).
[34] A.L. Pankratov, Appl. Phys. Lett., **92**, 082504 (2008).
[35] A.L. Pankratov, Phys. Rev. B, **78**, 024515 (2008).
[36] J. Dahm, A. Denestein, D.N. Langenberg, W.H. Parker, D. Rogovin, and D.J. Scalapino, Phys. Rev. Lett. **22**, 1416 (1969).
[37] E. Joergensen, V.P. Koshelets, R. Monaco, J. Mygind, M.R. Samuelsen, and M. Salerno, Phys. Rev. Lett. **49**, 1093 (1982).
[38] A.N. Malakhov, *Fluctuations in Autooscillating Systems*,

(Science, Moscow, 1968) (in Russian).